Compact TDLAS based sensor design using interband cascade lasers for mid-IR trace gas sensing

Lei Dong,[1,2,3,*] Frank K. Tittel,[3]Chunguang Li,[3] Nancy P. Sanchez,[4] Hongpeng Wu,[1,2,3] Chuantao Zheng,[3] Yajun Yu,[3] Angelo Sampaolo,[3,5] and Robert J. Griffin[4]

[1]*State Key Laboratory of Quantum Optics and Quantum Optics Devices, Institute of Laser Spectroscopy, Shanxi University, Taiyuan 030006, China*

[2]*Collaborative Innovation Center of Extreme Optics, Shanxi University, Taiyuan 030006, China*

[3]*Department of Electrical and Computer Engineering, Rice University, 6100 Main Street, Houston, TX 77005, USA*

[4]*Department of Civil and Environmental Engineering, Rice University, Houston, Texas 77005, USA*

[5]*Dipartimento Interateneo di Fisica, Università e Politecnico di Bari, CNR-IFN UOS BARI, Via Amendola 173, Bari, Italy*

[*]*donglei@sxu.edu.cn*

Abstract: Two compact TDLAS sensor systems based on different structural optical cores were developed. The two optical cores combine two recent developments, gallium antimonide (GaSb)-based ICL and a compact multipass gas cell (MPGC) with the goal to create compact TDLAS based sensors for the mid-IR gas detection with high detection sensitivity and low power consumption. The sensors achieved minimum detection limits of ~5 ppbv and ~8 ppbv, respectively, for CH_4 and C_2H_6 concentration measurements with a 3.7-W power consumption.

OCIS codes: (280.3420) Laser sensors; (140.5965) Semiconductor lasers, quantum cascade; (300.6340) Spectroscopy, infrared.

References and links

1. H. I. Schiff, G. I. Mackay, and J. Bechara, "The use of tunable diode laser absorption spectroscopy for atmospheric measurements," Res. Chem. Intermed. **20**(3-5), 525–556 (1994).
2. K. Krzempek, R. Lewicki, L. Nähle, M. Fischer, J. Koeth, S. Belahsene, Y. Rouillard, L. Worschech, and F. K. Tittel, "Continuous wave, distributed feedback diode laser based sensor for trace gas detection of ethane," Appl. Phys. B **106**(2), 251–255 (2012).
3. M. Köhring, S. Huang, M. Jahjah, W. Jiang, W. Ren, U. Willer, C. Caneba, L. Yang, D. Nagrath, W. Schade, and F. K. Tittel, "QCL based TDLAS sensor for detection of NO towards emission measurements from ovarian cancer cells," Appl. Phys. B **117**(1), 445–451 (2014).
4. B. H. Lee, E. C. Wood, M. S. Zahniser, J. B. McManus, D. D. Nelson, S. C. Herndon, G. W. Santoni, S. C. Wofsy, and J. W. Munger, "Simultaneous measurement of atmospheric HONO and NO2 via absorption spectroscopy using tunable mid-infrared contimuous-wave quantum cascade lasers," Appl. Phys. B **102**, 417–423 (2011).
5. J. B. McManus, M. S. Zahniser, D. D. Nelson, J. H. Shorter, S. Herndon, E. Wood, and R. Wehr, "Application of quantum cascade lasers to high-precision atmospheric trace gas measurements," Opt. Eng. **49**(11), 111124 (2010).
6. K. Liu, L. Wang, T. Tan, G. Wang, W. Zhang, W. Chen, and X. Gao, "Highly sensitive detection of methane by near-infrared laser absorption spectroscopy using a compact dense-pattern multipass cell," Sensor Actuat. B **220**, 1000–1005 (2015).
7. G. Durry, J. S. Li, I. Vinogradov, A. Titov, L. Joly, J. Cousin, T. Decarpenterie, N. Amarouche, X. Liu, B. Parvitte, O. Korablev, M. Gerasimov, and V. Zéninari, "Near infrared diode laser spectroscopy of C_2H_2, H_2O, CO_2 and their isotopologues and the application to TDLAS, a tunable diode laser spectrometer for the martian PHOBOS-GRUNT space mission," Appl. Phys. B **99**(1-2), 339–351 (2010).
8. S. Suchalkin, G. Belenky, and M. A. Belkin, "Rapidly tunable quantum cascade lasers," IEEE J. Sel. Top. Quantum Electron. **21**(6), 1200509 (2015).
9. I. Vurgaftman, W. W. Bewley, C. L. Canedy, S. K. Chul, K. Mijin, C. D. Merritt, J. Abell, and J. R. Meyer, "Interband cascade lasers with low threshold power and high output powers," IEEE J. Sel. Top. Quantum Electron. **19**(4), 1200210 (2013).
10. A. Bauer, F. Langer, M. Dallner, M. Kamp, M. Motyka, G. Sek, K. Ryczko, J. Misiewicz, S. Höfling, and A. Forchel, "Emission wavelength tuning of interband cascade lasers in the 3-4 μm spectral range,"," Appl. Phys. Lett. **95**(25), 251103 (2009).

#257497 Received 18 Jan 2016; revised 16 Feb 2016; accepted 17 Feb 2016; published 25 Feb 2016

11. C. L. Canedy, C. S. Kim, C. D. Merritt, W. W. Bewley, I. Vurgaftman, J. R. Meyer, and M. Kim, "Interband cascade lasers with >40% continuous-wave wall plug efficiency at cryogenic temperatures," Appl. Phys. Lett. **107**(12), 121102 (2015).
12. L. Nähle, L. Hildebrandt, M. Kamp, and S. Höfling, "ICLs open opportunities for mid-IR sensing," Laser Focus World **49**, 70–73 (2013).
13. L. Hidebrandt and L. Nähle, "DFB laser diodes expand hydrocarbon sensing beyond 3 μm," Laser Focus World **48**, 87–90 (2012).
14. T. Nguyen Ba, M. Triki, G. Desbrosses, and A. Vicet, "Quartz-enhanced photoacoustic spectroscopy sensor for ethylene detection with a 3.32 μm distributed feedback laser diode," Rev. Sci. Instrum. **86**(2), 023111 (2015).
15. I. Vurgaftman, W. W. Bewley, C. L. Canedy, C. S. Kim, M. Kim, C. D. Merritt, J. Abell, J. R. Lindle, and J. R. Meyer, "Rebalancing of internally generated carriers for mid-infrared interband cascade lasers with very low power consumption," Nat. Commun. **2**, 585 (2011).
16. K. Krzempek, M. Jahjah, R. Lewicki, P. Stefanski, S. So, D. Thomazy, and F. K. Tittel, "CW DFB RT diode laser based sensor for trace-gas detection of ethane using novel compact multipass gas absorption cell," Appl. Phys. B **112**(4), 461–465 (2013).
17. G. Overton, "New multipass gas cells beat conventional designs," Laser Focus World **49**, 17 (2013).
18. I. Bamberger, J. Stieger, N. Buchmann, and W. Eugster, "Spatial variability of methane: attributing atmospheric concentrations to emissions," Environ. Pollut. **190**, 65–74 (2014).
19. F. A. Smith, S. Elliott, D. R. Blake, and F. S. Rowland, "Spatiotemporal variation of methane and other trace hydrocarbon concentration in the Valley of Mexico," Environ. Sci. Policy **5**(6), 449–461 (2002).
20. I. J. Simpson, F. S. Rowland, S. Meinardi, and D. R. Blake, "Influence of biomass burning during recent fluctuations in the slow growth of global tropospheric methane," Geophys. Res. Lett. **33**(22), L22808 (2006).
21. Y. Xiao, J. A. Logan, D. J. Jacob, R. C. Hudman, R. Yantosca, and D. R. Blake, "Global budget of ethane and regional constraints on U.S. sources," J. Geophys. Res. **113**(D21), D2130 (2008).
22. K. Sun, L. Tao, D. J. Miller, M. Amir Khan, and M. A. Zondlo, "Inline multi-harmonic calibration method for open-path atmospheric ammonia measurement," Appl. Phys. B **110**(2), 213–222 (2013).
23. L. Tao, K. Sun, D. J. Miller, D. Pan, L. M. Golston, and M. A. Zondlo, "Low-power, open-path mobile sensing platform for high-resolution measurements of greenhouse gases and air pollutants," Appl. Phys. B **119**(1), 153–164 (2015).
24. D. Rehle, D. Leleux, M. Erdelyi, F. Tittel, M. Fraser, and S. Friedfeld, "Ambient formaldehyde detection with a laser spectrometer based on difference-frequency generation in PPLN," Appl. Phys. B **72**(8), 947–952 (2001).
25. M. Seiter and M. W. Sigrist, "On-line multicomponent trace-gas analysis with a broadly tunable pulsed difference-frequency laser spectrometer," Appl. Opt. **38**(21), 4691–4698 (1999).
26. C. Li, L. Dong, C. Zheng, and F. K. Tittel, "Compact TDLAS based optical sensor for ppb-level ethane detection by use of a 3.34 μm room-temperature CW interband cascade laser," Sens. Actuators B Chem. submitted.

1. Introduction

Numerous diverse applications of trace gas sensing includes environmental monitoring, industrial process control and the monitoring of gas concentrations at industrial locations, or exhaled breath for medical diagnostics. In all these applications, a fast, accurate and precise measurement of small concentrations of various trace gases is essential. Tunable diode laser absorption spectroscopy (TDLAS) is a versatile technique for real-time analysis of gas compositions, due to the fact that it offers narrow spectral resolutions, which permits unambiguous measurements of trace gas mixtures [1–4]. To-date trace gas species can be detected with sensitivities at ppt concentration levels using TDLAS [5]. The performance of TDLAS based sensors is dependent on the availability of suitable laser sources, such as single mode, distributed feedback (DFB) laser diodes in the near-infrared (near-IR) wavelength up to ~3 μm [6,7], quantum cascade lasers (QCLs) in the mid-infrared (mid-IR) region beyond ~3.7 μm [8] and GaSb-based interband cascade lasers (ICLs) emitting in the 3-4 μm wavelength range. The commercial availability of ICLs in 2009 led to new opportunities for TDLAS based sensing applications, especially the detection of hydrocarbons [9–14]. Hydrocarbons, such as methane (CH_4), ethane (C_2H_6), propane (C_3H_8), ethylene (C_2H_4), propene (C_3H_6), acetylene (C_2H_2), have strong absorption features in the 3-4 μm spectral range where their fundamental absorption band is located. Furthermore, ICLs have a reduced size, operate in a continuous-wave (CW) mode at room temperature with low power consumption levels [15],

TDLAS based sensors significantly depend on the footprint of the multi-pass gas cell (MPGC) and the associated gas handling system. A novel design of an astigmatic MPGC, developed by Sentinel Photonics/Aeris Technologies in 2013, resulted in a significantly reduced footprint [16,17]. The MPGC design employs two concave spherical mirrors using a

#257497 Received 18 Jan 2016; revised 16 Feb 2016; accepted 17 Feb 2016; published 25 Feb 2016

more complex dense spot pattern than the typical traditional circular or elliptical beam patterns in conventional MPGCs, such as a Herriott MPGC, which minimizes the laser beam spot overlap and hence minimizes etalon fringe effects. The new MPGC design offers a 54.6-m path length in the 17 × 6.5 × 5.5 cm^3 package with a 220-ml sampling volume, which also allows reduced gas-exchange times.

The two TDLAS based optical sensors were employed to detect methane and ethane. Methane is a key contributor to the greenhouse effect and a safety hazard in several industries, including natural gas production and storage, transportation, coal mining as well as the handling of liquefied methane. The ability to monitor methane in urban and rural areas is important [18,19]. After methane, ethane is the second-largest component of natural gas which is used in the production of ethylene or in the manufacture of other commodity chemicals. Its concentration in ambient air strongly affects both atmospheric chemistry and climate. Hence the detection of ethane is of interest for environmental monitoring [20,21].

2. Sensor design

2.1 Optical core design with a two-floor structure

A CW, DFB ICL from Nanoplus GmbH, Germany employed in our sensor design is packaged in a 5 × 5 × 5 cm^3 TO66 assembly which includes a thermoelectric cooler (TEC). A TEC, mercury-cadmium-telluride (MCT) detectors from Vigo System S.A., configured with a preamplifier in a footprint of 40 × 81 × 40 mm^3 was used in our compact TDLAS sensor system. A beam mode matching lens of 200-mm focal length, with its focal point positioned at the MPGC entry port is required for optimum power transfer from the ICL source to the MPGC. A two-floor optical core architecture was adopted in order to accommodate the required optical components on a compact sensor platform, as shown in Fig. 1. The ICL, an alignment diode laser, and a dichroic mirror were mounted on the base plate (*Floor* 1). The visible laser beam from the alignment diode laser (λ = 630 nm) was aligned collinearly with the mid-IR beam by means of the dichroic mirror (ISO optics, model BSP-DI-25-3), as a guide beam to assist in the optical alignment of the sensor system. A 45 degree angle plane mirror (M1) directed the combined beams from the bottom floor (*Floor* 1) to the top floor (*Floor* 2). Another plane mirror (M2) converted the combined laser beams from a vertical to a horizontal propagation. The top plate accommodates the MPGC, the MCT detector and several other optical components, such as a lens and mirrors. Several dowel pins were used between the top and bottom floor to avoid optical misalignment. Using a mode matching lens (L), the beam was coupled into the MPGC. The plane mirrors, M3 and M4, folded the necessary optical path into a smaller space, since the focal point of the lens with a 200-mm focal length has to be positioned at the MPGC entry. The enclosure of the MPGC was made of super invar with a thermal expansion coefficient of 10^{-6}/°C. In addition, the enclosure of the MPGC has a gas inlet and outlet. After 435 beam passes, the collimated ICL beam exiting the MPGC was focused onto a TEC, MCT detector using a plane mirror (M5) and a 35 mm focal length parabolic mirror.

#257497 Received 18 Jan 2016; revised 16 Feb 2016; accepted 17 Feb 2016; published 25 Feb 2016

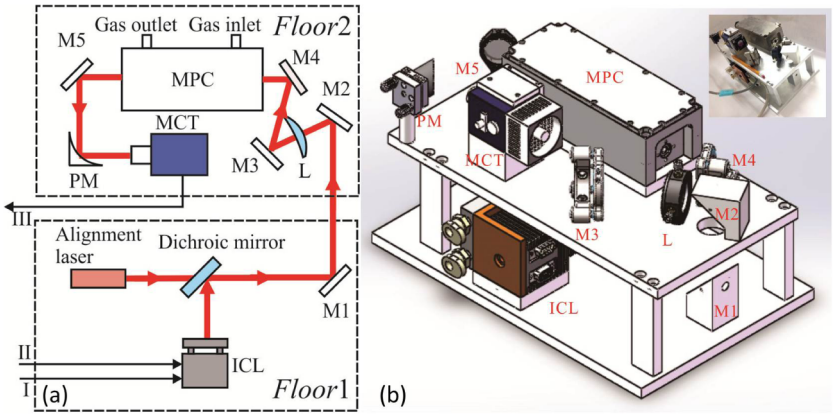

Fig. 1. (a) Schematic of the sensor depicts the two-floor optical core. (b) CAD image of the optical core with dimensions of length (32 cm), width (20 cm), and height (17 cm). Inserted image: photograph of the two-floor optical core. ICL: interband cascade laser; L: lens; M: plane mirror; MCT: mercury-cadmium-telluride detector; MPGC: multi-pass gas cell; PM: parabolic mirror.

To further assist heat dissipation, a custom made copper heat exchanger was attached on the ICL heat sink, which was connected to a compact water chiller (Solid State Cooling system, Oasis 160). The chiller is used, when the sensor system is operated at high ambient temperatures (>40°C). The photograph of the two-floor optical core is shown in the insert of Fig. 1(b).

2.2 Optical core design with a single-floor structure

To further minimize the sensor size, we designed a second-generation sensor optical core with a single-floor structure using almost identical optical components with those of the two-floor optical sensor core, as shown in Fig. 2. In the single-floor design, the 630 nm alignment diode laser was mounted on a separated daughter board since it is not necessary for the alignment laser to be present after completing the optical collimation of the sensor system. The daughter board can be positioned on the main board by means of two dowel pins. An adjustable iris was placed in front of the alignment laser on the daughter board for beam shaping. The main board incorporates the ICL, MPGC, MCT detector and auxiliary optical components. After the mid-IR ICL beam and the visible beam from the alignment laser were aligned collinearly by means of a dichroic mirror, the combined beam was coupled into the MPGC using a mode matching lens. Two plane mirrors, M1 and M2, converted the laser beam direction by 180 degrees to provide the required 200-mm distance for the mode matching lens, folding the optical path and reducing the size of the sensor optical core. The collimated ICL beam exiting the MPGC was focused onto the TEC, MCT detector using a 35 mm focal length parabolic mirror. In addition, an improved design feature of the sensor optical core is that an in-line reference cell can be inserted between the ICL and the dichroic mirror [22,23]. This can provide a reference signal to identify the laser wavelength in real time and avert a wavelength drift, when target gases are not present. A pressure controller (Bronkhorst, Netherlands) was added on the main board to control the gas pressure in the MPGC. Furthermore, in most cases the water chiller was not used and the ICL was operated in a temperature range between 25°C and 35°C. The custom-made copper heat exchanger was not included in the single-board design. The photograph of the single-floor optical core is shown in the insert of Fig. 2(b).

#257497 Received 18 Jan 2016; revised 16 Feb 2016; accepted 17 Feb 2016; published 25 Feb 2016

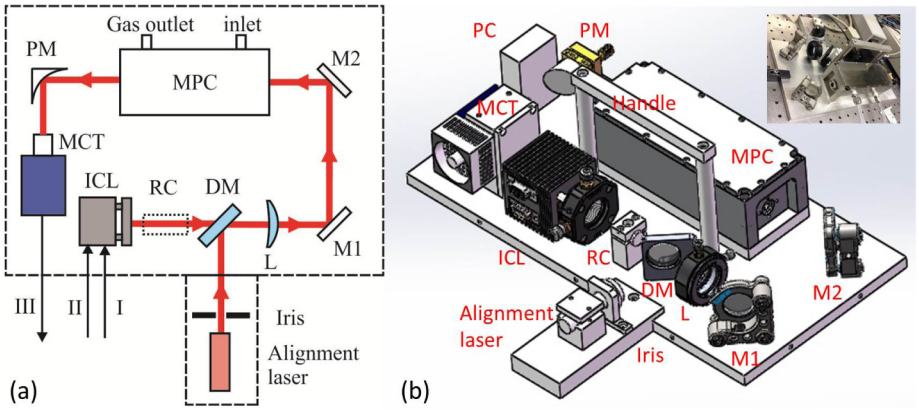

Fig. 2. (a) Schematic of the sensor optical core based on a single-floor structure. (b) CAD image of the optical core with reduced dimensions of length (35.5 cm), width (18 cm), and height (8 cm). Inserted image: photograph of a single-floor optical core. ICL: interband cascade laser; DM: dichroic mirror; L: lens; M: plane mirror; MCT: mercury-cadmium-telluride detector; MPGC: multi-pass gas cell; PM: parabolic mirror; RC: reference cell.

2.3 Control unit and data processing

The two sensor optical cores have an identical control unit as shown in Fig. 3, since both are based on TDLAS. The temperature controller was programmed to control the ICL temperature. A current driver provides the ICL driving current. In order to minimize the dimension of the control unit, a compact, low-noise laser driver board developed by NEO Monitors, SA, Norway was selected. The laser driver has a size of 10 cm × 8 cm with low noise current characteristics of ≤1 nA/√Hz and an on-board TEC driver (± 3 A, 15 V). A laptop equipped with a NI DAQ card (NI 6062 E) was used to generate the 500 Hz sawtooth wave with a DC offset. The offset determines the ICL center wavelength, while the sawtooth wave is used to scan the ICL wavelength center wavelength. The amplitude of the offset depends on the characterization of the ICL and the wavelength of the target absorption line. The laptop DAQ combination acquired the spectral data from the MTC detector with a sampling rate of 250 kS/s.

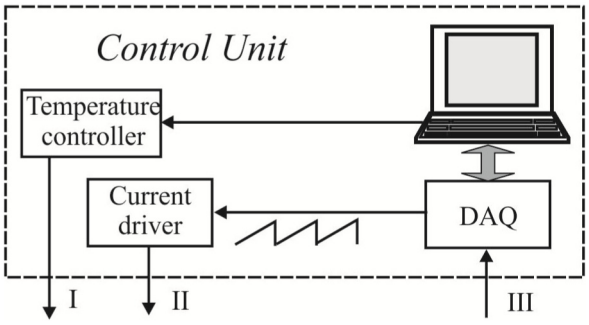

Fig. 3. Schematic of control unit of the TDLAS based sensor system.

The data processing is performed as follows. First, 150 spectra were averaged by ramping the laser current at 500 Hz to cover the targeted spectral region and collecting the detector output using the DAQ. Every spectrum incorporates 500 data points. In order to obtain the baseline of a spectral scan, the absorption peak was removed from the averaged spectrum. Subsequently, the remaining data points were fitted by means of a fifth order polynomial, as shown in Fig. 4(a). On the basis of fitting the baseline, the absorbance can be calculated, which was then linearized using the quadratic polynomial obtained in advance from the fringe spacing of a Ge etalon. Finally, a Voigt line shape was fitted to the linearized absorbance using a

#257497 Received 18 Jan 2016; revised 16 Feb 2016; accepted 17 Feb 2016; published 25 Feb 2016

Levenberg-Marquardt least-squares fit procedure to retrieve the target gas concentrations, as described in [24]. The output rate of the concentration is 1 Hz.

The maximum TEC power consumption is 3 W. A 12-V power supply was used due to the compatibility with car batteries. With a maximum laser current of 60 mA, the ICL requires a 0.72-W power. Hence the total power consumption for the sensor optical core is ~3.7 W.

3. Performance assessment of single- and two-floor optical cores

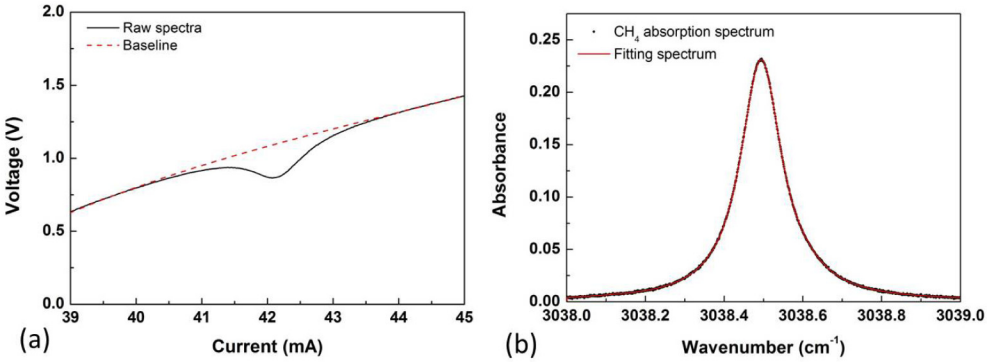

Fig. 4. (a) CH_4 absorption line at 3038.5 cm^{-1} with a fitting baseline. (b) Calculated linearized absorbance as a function of wavenumber with a Voigt line shape fitting.

The TDLAS based sensor based on the two-floor optical core was configured with an ICL with a center wavelength of 3291 nm for methane detection. An interference-free methane line located at 3038.5 cm^{-1} was selected as the target line to perform methane detection in ambient air [25]. The ICL temperature was set to 30 °C by the TEC driver. A DC offset of 2.1 V enables the current driver to provide a constant current of 42 mA. The ICL output power is 1.5 mW. A sawtooth wave with amplitude of 0.4 V results in an ICL current scan from 39 mA to 45 mA, corresponding to a wavelength range from 3038 cm^{-1} to 3039 cm^{-1}. A typical 150-averaging raw methane spectrum acquired from laboratory air is depicted in Fig. 4(a) together with a fitted baseline. The absorbance as a function of wavelengths was calculated and linearized by means of a 2.54 cm long Germanium etalon with a free spectral range of 1.44 GHz, as shown in Fig. 4(b). The Voigt line shape was fitted to retrieve the concentration information. In this manner, a methane concentration value of 4 ppm was obtained.

The TDLAS based sensor based on the single-floor optical core was configured with a 3337 nm ICL for ethane detection. The 2996.88 cm^{-1} absorption line, interference free from other atmospheric gases, was used for the C_2H_6 sensor system [26]. The ICL was operated at a current of 47 mA and temperature of 10°C, which provides an optical power of ~8 mW. The pressure in the MPGC was reduced to 100 Torr in order to avoid spectral overlap. A sawtooth wave scan of the ICL current from 46.3 mA to 47.7 mA, results in wavelength tuning between 2996.76 cm^{-1} to 2996.94 cm^{-1}. A typical 150-averaging raw C_2H_6 spectrum acquired from a known concentration level of 30 ppbv is depicted in Fig. 5(a) together with a fitting baseline. A standard C_2H_6/N_2 mixture was obtained from a standard gas generator (Environics, Series 4040). Figure 5(b) shows the linearized absorbance and the fitting spectrum, which yields a measured value of 32 ppbv.

#257497 Received 18 Jan 2016; revised 16 Feb 2016; accepted 17 Feb 2016; published 25 Feb 2016

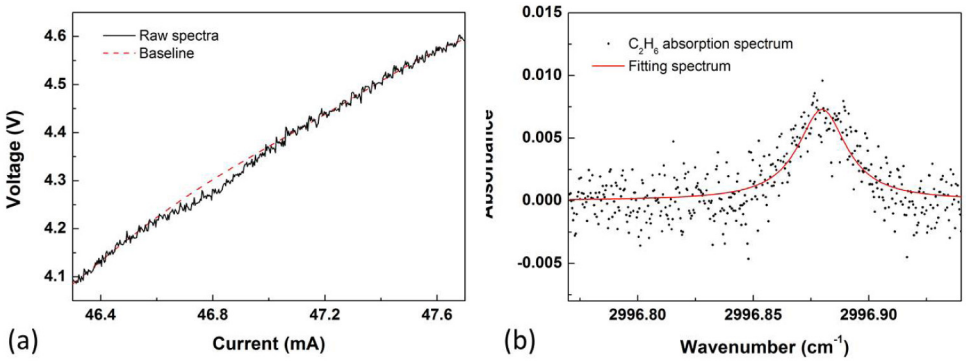

Fig. 5. (a) Raw C_2H_6 absorption line at 2996.88 cm^{-1} with a fitting baseline. (b) Calculated linearized absorbance of C_2H_6 as a function of wavenumber with a Voigt line shape fitting.

In order to obtain the detection limit of the two TDLAS sensor systems, pure nitrogen was introduced into the two sensor systems. With an integration time of 1 sec., a detection limit of ~5 ppbv was achieved for a CH_4 measurement, while a detection limit of ~8 ppbv was obtained for a C_2H_6 measurement.

The TDLAS based CH_4 sensor system based on the two-floor optical core was deployed in a compact vehicle (Toyota Prius) to evaluate its performance for atmospheric methane monitoring. The vehicle was driven from the Rice University campus initially in the Greater Houston area monitoring CH_4 and ending up ~24 miles at the perimeter of a compressed natural gas (CNG) station. Figure 6 shows the CH_4 levels detected at the Clean Energy CNG O'Rourke Station (with GPS coordinates: 29°47′10"N 95°16′49"W). The vehicle stayed there for ~10 mins from 11:09-11:19 am on December 22, 2015. An increase in the CH_4 mixing ratios compared with the observed background levels (~1.8 ppm) was noticed while the vehicle was stationary at this location. Methane concentrations as high as ~5 ppm were detected in the vicinity of the CNG station, indicating that CH_4 levels 3 times as large as the atmospheric background level occurred at this location.

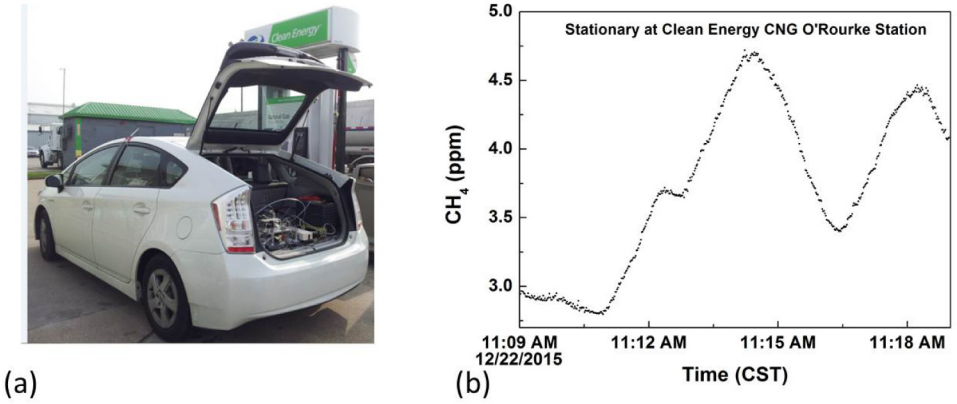

Fig. 6. (a) Photograph of vehicle mounted with a compact TDLAS based CH_4 sensor system at a Clean Energy compressed natural gas (CNG) station operated by O'Rourke in northwest Houston, TX. (b) CH_4 concentrations measured at the Clean Energy CNG O'Rourke Station for a ~10 minute sampling period.

4. Conclusions

We designed and tested two TDLAS based sensor optical cores with two-floor and single-floor structures, respectively. Both optical cores employed a CW, room temperature, ICL and a

#257497 Received 18 Jan 2016; revised 16 Feb 2016; accepted 17 Feb 2016; published 25 Feb 2016

compact MPGC, in order to evaluate the performance of both sensitive and selective mid-IR TDLAS based trace gas sensor systems with low electrical power consumption. With a three dimensional folded optical path design, the optical core with a two-floor structure has a footprint of 32 × 20 × 17 cm^3. An improved version with a single-floor structure, based on modular design method, reduced the footprint to a ~half of the two-floor version (35.5 × 18 × 8 cm^3). The two TDLAS based sensor systems were used for CH_4 and C_2H_6 concentration measurements, respectively. The results demonstrated a ppb-level detection sensitivity for C_2H_6 and CH_4 trace measurements. The main electrical power consumption was due to the 50-W laptop. A future sensor upgrade will employ an ARM microprocessor-based controller, instead of the laptop with NI DAQ card, which will have a significantly smaller size, lower power consumption and longer battery life.

Acknowledgments

Lei Dong acknowledges support by the 973 program (Grant No. 2012CB921603), National Natural Science Foundation of China (Grant #s. 61575113, 61275213). Frank Tittel, Nancy Sanchez, and Robert Griffin acknowledge support by the National Science Foundation (NSF) ERC MIRTHE award. Frank Tittel acknowledges support by the Robert Welch Foundation (Grant C-0586) and two Department of Energy ARPA-E awards DE-AR0000545 and DE-AR000053.

#257497 Received 18 Jan 2016; revised 16 Feb 2016; accepted 17 Feb 2016; published 25 Feb 2016